

**Intervalence Charge Transfer in a “Chain-like”
Ruthenium Trinuclear Assembly based on the
Bridging Ligand 4,7-phenanthroline-5,6:5',6'-pyrazine (ppz)**

Deanna M. D'Alessandro and F. Richard Keene*

SUPPLEMENTARY INFORMATION

Table S1. ^1H Chemical shifts (ppm) for Λ - $[\text{Ru}(\text{bpy})(\text{HAT})_2]^{2+}$ and Λ^t - $[\text{Ru}(\text{bpy})(\text{ppz})_2]^{2+}$ (CD_3CN , PF_6^- salts). The ^1H NMR spectra of the Δ and Λ enantiomers were identical in each case.

		$[\text{Ru}(\text{bpy})(\text{HAT})_2]^{2+}$	<i>trans</i> - $[\text{Ru}(\text{bpy})(\text{ppz})_2]^{2+}$
bpy ^a	H3	8.60	8.58
	H4	8.16	8.14
	H5	7.39	7.34
	H6	7.83	7.83
HAT	H2	8.39 (2H, $J = 3$ Hz, d)	
	H3	9.24 (2H, s)	
	H6	9.39 (2H, s)	
	H7	9.39 (2H, s)	
	H10	9.02 (2H, s)	
	H11	8.29 (2H, $J = 3$ Hz, d)	
ppz	H2		8.86 (2H, $J = 3$ Hz, d)
	H3		8.11 (2H, $J = 3$ Hz, d)
	H6		8.22 (2H, $J = 5, 1$ Hz, dd)
	H7		7.97 (2H, $J = 10, 8$ Hz, dd)
	H8		9.32 (2H, $J = 8$ Hz, d)
	H9		9.32 (2H, $J = 8$ Hz, d)
	H10		8.11 (2H, $J = 10, 8$ Hz, dd)
	H11		9.26 (2H, $J = 3, 1.5$ Hz, dd)

^a H6 (2H, $J = 5, 1.5$ Hz, dd); H5 (2H, $J = 8, 5$ Hz, dd); H4 (2H, $J = 8, 8$ Hz, dd); H3 (2H, $J = 8, 1.5$ Hz, dd).

Table S2. ^1H chemical shifts (ppm) for $\Delta\Delta^t\Delta\text{-}[\{\text{Ru}(\text{bpy})_2\}_2\{\text{Ru}(\text{bpy})(\mu\text{-ppz})_2\}]^{6+}$ by comparison with the *meso*- and *rac*- $[\{\text{Ru}(\text{bpy})_2\}_2(\mu\text{-ppz})]^{4+}$ (CD_3CN , PF_6^- salts).

		<i>meso</i> ($\Delta\Delta/\Delta\Delta$)	<i>rac</i> ($\Delta\Delta/\Delta\Delta$)	$\Delta\Delta^t\Delta$
bpy ring a ^a (over bpy)	H3'	8.58	8.53	8.59
	H4'	8.15	8.13	8.20
	H5'	7.50	7.51	7.52
	H6'	7.73	7.76	7.77
bpy ring b ^a (over ppz)	H3	8.52	8.51	8.50
	H4	8.09	8.07	8.10
	H5	7.39	7.02	7.17
	H6	7.85	7.61	7.42
bpy ring c ^a (over bpy)	H3'	8.43	8.55	8.53
	H4'	8.06	8.15	8.20
	H5'	7.42	7.38	7.36
	H6'	7.75	7.66	7.65
bpy ring d ^a (over ppz)	H3	8.39	8.48	8.53
	H4	7.99	8.00	8.07
	H5	7.25	7.36	7.20
	H6	7.54	7.42	7.65
bpy ring e ^a (over ppz)	H3			8.53
	H4			8.02
	H5			7.36
	H6			7.47
ppz ^b	H2	7.93 (H2/3)	7.96 (H2/3)	7.98
	H3			8.08
	H6	8.23 (H6/11)	8.23 (H6/11)	8.25
	H7	8.01 (H7/10)	8.01 (H7/10)	8.10
	H8	9.32 (H8/9)	9.31 (H8/9)	9.36
	H9			9.33
	H10			8.03
H11			8.09	

^a H6 (dd; $J = 5, 1.5$ Hz); H5 (dd; $J = 8, 5$ Hz); H4 (dd; $J = 8, 8$ Hz); H3 (dd; $J = 8, 1.5$ Hz).

^b H2/3 (s); H 6/11 (dd, $J = 5, 1.5$ Hz); H7/10 (dd, $J = 10, 8$ Hz); H8/9 (dd, $J = 8, 1.5$ Hz).

Table S3. Ligand-based reduction potentials^a data (in mV), and K_c values^b for the di- and trinuclear complexes in 0.1 M [(*n*-C₄H₉)₄N]PF₆/CH₃CN at +25°C. The potentials for [Ru(bpy)₃]²⁺ are included for comparison.

Complex	E _{red1}	E _{red2}	E _{red3}	E _{red4}
[Ru(bpy) ₃] ²⁺	-1717	-1912	-2160	-2700
<i>trans</i> -[Ru(bpy)(ppz) ₂] ²⁺ ^c	-1000	-1246	-1700	-1968 ^b
<i>meso</i> -[{Ru(bpy) ₂ } ₂ (μ-ppz)] ⁴⁺	-956	-1704	-1890	-1956
<i>rac</i> -[{Ru(bpy) ₂ } ₂ (μ-ppz)] ⁴⁺	-944	-1696	-1878	-1975
ΔΔ ^t Δ- [{Ru(bpy) ₂ } ₂ {Ru(bpy)(μ-ppz) ₂ }] ⁶⁺	-868	-1036	-1800 ^b	-2072 ^b

^a All potentials (± 3 mV) in 0.1 M [(*n*-C₄H₉)₄N]PF₆/CH₃CN at +25°C vs. Fc⁺/Fc⁰.

^b Two-electron reduction process.

^c The redox properties of the Δ and Λ enantiomers were identical.

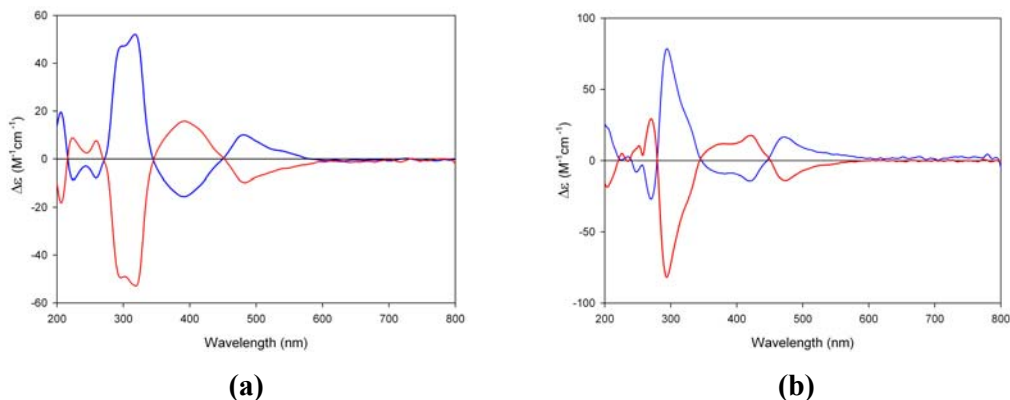


Figure S1. CD spectra (CH₃CN) of **(a)** Δ- and Λ-[Ru(bpy)(HAT)₂]²⁺, Band 1 (Δ): (—) and Band 2 (Λ): (—); **(b)** Δ^t- and Λ^t-[Ru(bpy)(ppz)₂]²⁺, Band 1 (Δ) (—) and Band 4 (Λ): (—).

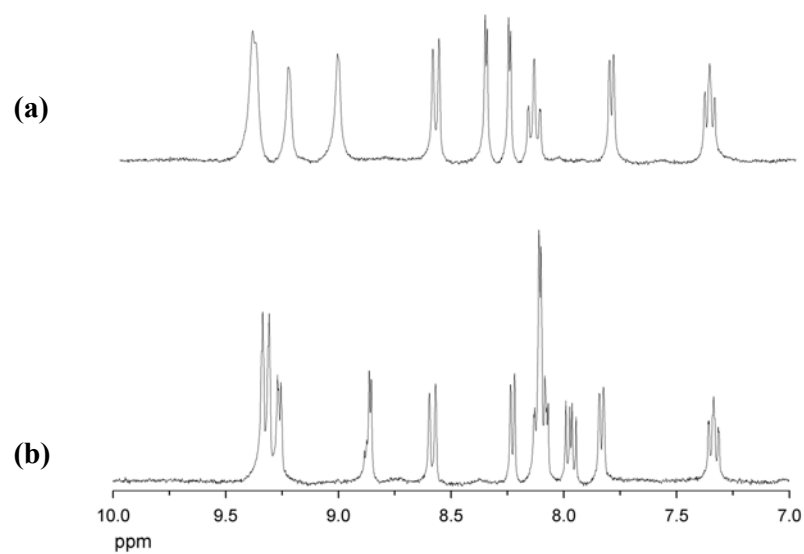


Figure S2. ^1H NMR spectra of (a) Λ - $[\text{Ru}(\text{bpy})(\text{HAT})_2]^{2+}$ and (b) Λ^t - $[\text{Ru}(\text{bpy})(\text{ppz})_2]^{2+}$ (CD_3CN , PF_6^- salts).

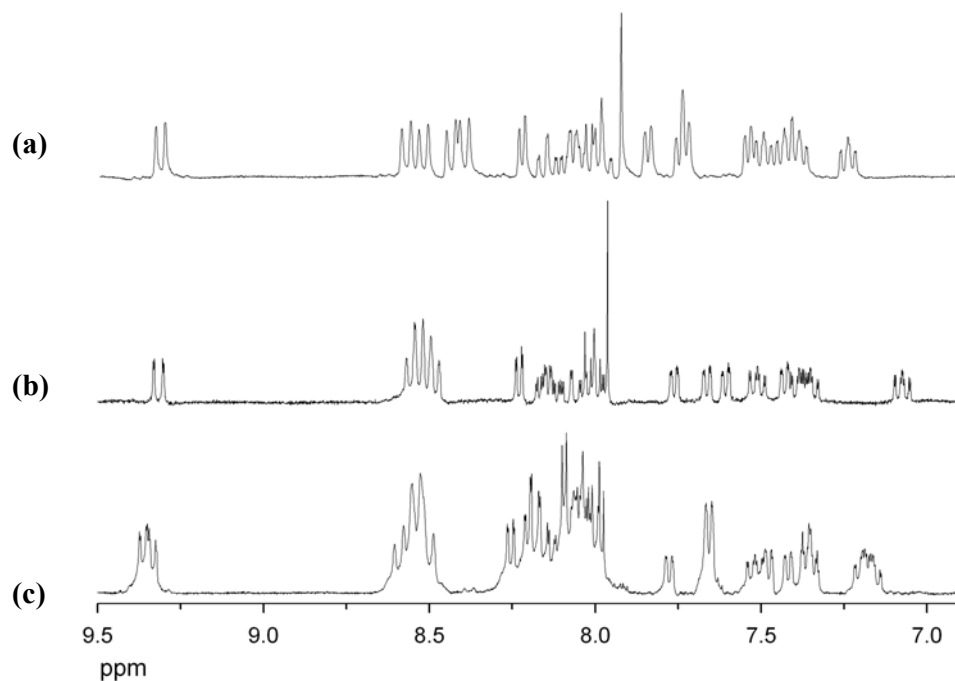


Figure S3. ^1H NMR spectra (CH_3CN) for **(a)** *meso*- and **(b)** *rac*- $[\{\text{Ru}(\text{bpy})_2\}_2(\mu\text{-ppz})]^{4+}$, and **(c)** $\Delta\Delta^1\Delta$ - $[\{\text{Ru}(\text{bpy})_2\}_2\{\text{Ru}(\text{bpy})(\mu\text{-ppz})_2\}]^{6+}$ (CD_3CN , PF_6^- salts).

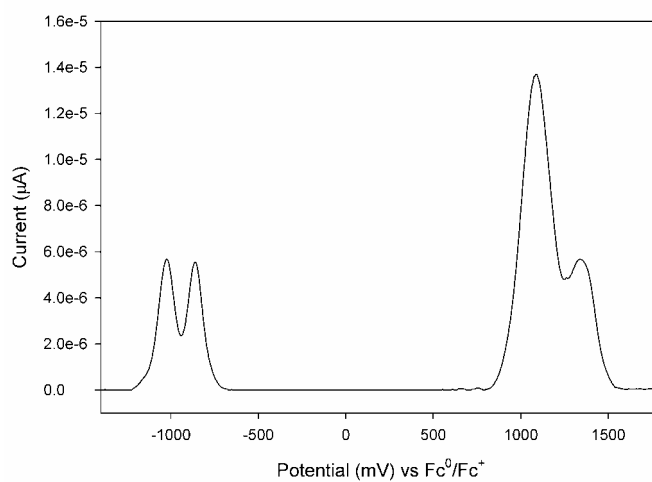


Figure S4. Differential Pulse Voltammogram of $\Delta\Delta^t\Delta^-$ [$\{\text{Ru}(\text{bpy})_2\}_2\{\text{Ru}(\text{bpy})(\mu\text{-ppz})_2\}$] $^{6+}$ in 0.1 M $[(n\text{-C}_4\text{H}_9)_4\text{N}]\text{PF}_6/\text{CH}_3\text{CN}$ at +25°C.

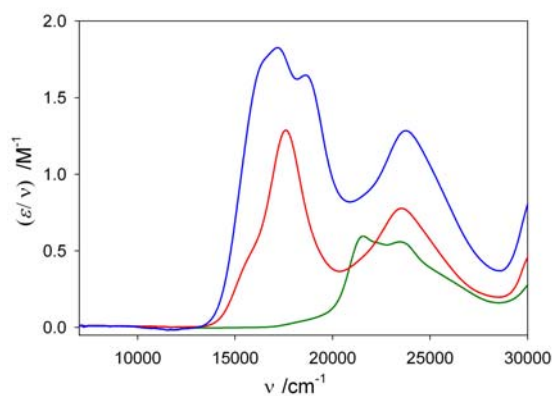


Figure S5. UV/Vis/NIR spectra of $[\text{Ru}(\text{bpy})(\text{ppz})_2]^{2+}$ (———), *meso*- $[\{\text{Ru}(\text{bpy})_2\}_2(\mu\text{-ppz})]^{4+}$ (———) and $\Delta\Delta^t\Delta^-$ - $[\{\text{Ru}(\text{bpy})_2\}_2\{\text{Ru}(\text{bpy})(\mu\text{-ppz})_2\}]^{6+}$ (———) in CH_3CN at $+25^\circ\text{C}$.

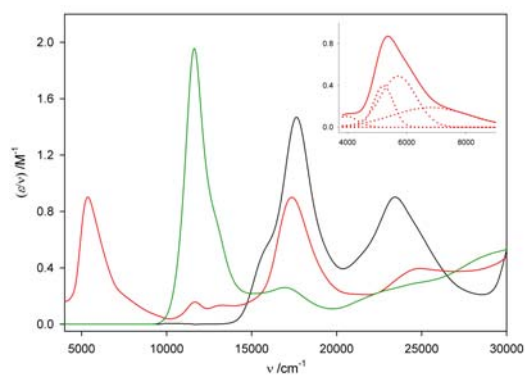


Figure S6. UV/Vis/NIR spectra of *meso*- $[\{\text{Ru}(\text{bpy})_2\}_2(\mu\text{-ppz})]^{n+}$ $\{n = 4$ (———), 5 (———), 6 (———) $\}$ at -35°C . The inset shows the best fit of the bands obtained by Gaussian deconvolution of the IVCT band.